Molecular Plant Pathology

MOLECULAR PLANT PATHOLOGY (2011) **12**(8), 715–730 DOI: 10.1111/J.1364-3703.2011.00706.X

Comparative analysis of the XopD type III secretion (T3S) effector family in plant pathogenic bacteria

JUNG-GUN KIM, KYLE W. TAYLOR AND MARY BETH MUDGETT*

Department of Biology, Stanford University, Stanford, CA 94305-5020, USA

SUMMARY

XopD is a type III effector protein that is required for *Xanthomonas campestris* pathovar *vesicatoria* (Xcv) growth in tomato. It is a modular protein consisting of an N-terminal DNA-binding domain, two ethylene-responsive element binding factor-associated amphiphilic repression (EAR) transcriptional repressor motifs and a C-terminal small ubiquitin-related modifier (SUMO) protease. In tomato, XopD functions as a transcriptional repressor, resulting in the suppression of defence responses at late stages of infection. A survey of available genome sequences for phytopathogenic bacteria revealed that XopD homologues are limited to species within three genera of Proteobacteria—*Xanthomonas*, *Acidovorax* and *Pseudomonas*. Although the EAR motif(s) and SUMO protease domain are conserved in all XopD-like proteins, variation exists in the length and sequence identity of the N-terminal domains. Comparative analysis of the DNA sequences surrounding *xopD* and *xopD-like* genes led to revised annotation of the *xopD* gene. Edman degradation sequence analysis and functional complementation studies confirmed that the *xopD* gene from Xcv encodes a 760-amino-acid protein with a longer N-terminal domain than previously predicted. None of the XopD-like proteins studied complemented Xcv Δ*xopD* mutant phenotypes in tomato leaves, suggesting that the N-terminus of XopD defines functional specificity. Xcv Δ*xopD* strains expressing chimeric fusion proteins containing the N-terminus of XopD fused to the EAR motif(s) and SUMO protease domain of the XopD-like protein from *X. campestris* pathovar *campestris* strain B100 were fully virulent in tomato, demonstrating that the N-terminus of XopD controls specificity in tomato.

INTRODUCTION

Xanthomonas campestris pathovar *vesicatoria* (Xcv) causes bacterial spot disease in tomato and pepper (Jones *et al*., 2000). Xcv is a Gram-negative bacterium that infects leaves and fruit, causing necrotic lesions and chlorosis, resulting in leaf abscission and fruit loss (Stall, 1995). Like other phytopathogenic xanthomonads, Xcv uses the type III secretion (T3S) system to manipulate host physiology to promote bacterial growth (Bonas *et al*., 1991). Xcv uses the T3S system to translocate approximately 35 effector proteins into host plant cells (White *et al*., 2009). Collectively, the effector proteome mediates Xcv colonization and adaptation to its host plants. How host specificity is achieved remains a fundamental question in effector biology. Biochemical studies on individual Xcv effectors, however, are providing important insight.

Several Xcv T3S effectors appear to function as classical virulence factors (e.g. AvrBs2, AvrBs3, XopN, AvrXv4 and AvrBsT) (White *et al*., 2009). They are required for both Xcv fitness and disease symptom development in infected leaves. For example, AvrBs3 is a member of the transcription activator-like (TAL) effector family that functions as a site-specific transcription factor to directly reprogramme host gene expression during infection (Kay *et al*., 2007; Römer *et al*., 2007). The modulation of host transcription affects immunity and developmental processes, leading to leaf hypertrophy and pustule formation (Marois *et al*., 2002). XopN, a HEAT-repeat-containing protein, interacts with a tomato atypical receptor kinase, TARK1, and suppresses pathogen-triggered immunity (PTI) at the early stages of infection (Kim *et al*., 2009). AvrXv4 and AvrBsT belong to the YopJ effector family, a group of cysteine proteases conserved amongst animal and plant pathogenic bacteria (Staskawicz *et al*., 2001). Members of this family possess ubiquitin protease activity, small ubiquitin-related modifier (SUMO) protease activity and/or acetyltransferase activity (Mukherjee *et al*., 2006; Roden *et al*., 2004; Rytkonen *et al*., 2007). AvrXv4 exhibits weak SUMO protease activity *in planta* (Roden *et al*., 2004), whereas the enzymatic activity of AvrBsT is not known. However, it is clear that AvrBsT affects defence responses in a number of plant species. AvrBsT alters phospholipid signalling, resulting in defence activation in *Arabidopsis sober1* mutants (Kirik and Mudgett, 2009), and suppresses PTI in tomato (Kim *et al*., 2010) and effector-triggered immunity (ETI) in pepper (Szczesny *et al*., 2010).

**Correspondence*: Email: mudgett@stanford.edu

By contrast, XopD is a unique virulence factor that promotes tolerance to Xcv strain 85-10 in infected host leaves (Kim *et al*., 2008). It is required for maximal Xcv multiplication, but does not promote disease symptom development. Rather, XopD action suppresses leaf chlorosis and necrosis, two phenotypes associated with PTI activation at the late stages of infection (Kim *et al*., 2008). Structure–function studies have shown that XopD is a modular protein containing an N-terminal DNA-binding domain (Kim *et al*., 2008), two internal ethylene-responsive element binding factor-associated amphiphilic repression (EAR) motifs ($^{L}/_{F}$DLN$^{L}/_{F}$XP) (Ohta *et al*., 2001) and a C-terminal SUMO protease domain (Chosed *et al*., 2007; Hotson *et al*., 2003). Accumulation of XopD in plant nuclear speckles (Hotson *et al*., 2003) correlates with reduced host defence transcription, reduced salicylic acid levels and higher chlorophyll levels in Xcv-infected leaves (Kim *et al*., 2008). Host targets for XopD have not yet been reported, but they are predicted to be sumoylated nuclear proteins associated with the regulation of host transcription. These data support the model that XopD functions as a repressor to suppress PTI and senescence-like processes triggered in Xcv-infected leaves.

Few phytopathogenic bacteria carry XopD-like proteins, bringing into question the function and evolution of this effector family in bacterial pathogenesis. In *Pseudomonas syringae* pv. *eriobotryae*, the XopD homologue PsvA (referred to here as $PsvA_{Pse}$) is encoded on a plasmid and is required for pathogen virulence in loquat (Kamiunten, 1990, 1999). By contrast, PsvA from *X. campestris* pv. *campestris* (Xcc) strain ATCC 33913 (referred to here as $PsvA_{XccATCC33913}$) is chromosomally encoded and is not required for virulence (Castaneda *et al*., 2005). The discrepancy in the requirement for XopD-like proteins in bacterial virulence is not clear. This prompted us to examine the gene structure for *xopD* and *xopD-like* genes in the available genomes of phytopathogenic bacteria. We speculated that the sequence variation and genomic context for these loci might be significantly different as a result of horizontal gene transfer, recombination and/or transposition.

Comparison of the XopD protein family in phytopathogenic bacteria indicated that several XopD-like proteins were actually much larger than XopD. Discrepancies in the literature and in our own unpublished work suggested that the original *xopD* gene might have been incorrectly annotated. For example, the following lines of evidence suggested that the XopD protein contained a longer N-terminal domain: (i) the upstream sequence of the *xopD* locus reported in the Xcv 85-10 genome paper (Thieme *et al*., 2005) was different from that reported for the cloning of the *xopD* gene (Noël *et al*., 2002); (ii) the genome annotation predicted a large chromosomal gap between the *xopD* gene and the upstream open reading frame (ORF), *XCV0436*; inspection of this intergenic region identified an alternative *xopD* transcriptional start site just downstream of *XCV0436*; (iii) Xcv Δ*xopD* mutant phenotypes could only be complemented with a DNA fragment containing the 3′ end of *XCV0436* and the annotated *xopD* gene (Kim *et al*., 2008), consistent with the hypothesis that an alternative *xopD* start site is located adjacent to the pathogen-inducible promoter (PIP)-box; (iv) protein gel blot analysis showed that the XopD protein expressed in Xcv 85-10 was significantly larger than the predicted protein size (61.3 kDa) (Noël *et al*., 2002). On the basis of these data, we have revised the annotation of the *xopD* gene and characterized the functional specificity of the respective XopD protein relative to the other known XopD-like homologues.

We report a comparative analysis of the XopD T3S effector family in phytopathogenic bacteria. DNA sequence analysis of *xopD* and *xopD-like* genes has provided new insight into the functional variation that exists between family members. We now provide genetic and biochemical evidence that XopD has a longer N-terminal domain that determines the functional specificity in tomato. Although XopD-like effectors share EAR motifs and SUMO protease activity, they do not complement Xcv Δ*xopD* mutant phenotypes, suggesting that each may play a specific role within the context of the respective bacterial–host interaction.

RESULTS

Revised annotation of the *xopD* locus in Xcv strain 85-10

We hypothesized that XopD is a larger protein than originally predicted, containing a longer N-terminal domain. To investigate this, we reviewed the original annotation of the Xcv strain 85-10 genome sequence (Thieme *et al*., 2005). A large chromosomal gap was predicted between the putative *xopD* gene and the upstream ORF, *XCV0436* (Fig. 1A, top panel). The putative start site (ATG codon) for the *xopD* gene was annotated just downstream of an *hrp* box, a motif often found in the promoters of T3S system-associated genes in *Pseudomonas* spp. (Innes *et al*., 1993). The corresponding *xopD* ORF was predicted to encode a 545-amino-acid polypeptide (Fig. 1A) with a molecular weight of 61.3 kDa (Noël *et al*., 2002; Thieme *et al*., 2005). Intriguingly, a putative PIP-box was subsequently identified in the intergenic region between *XCV0436* and *xopD* (Koebnik *et al*., 2006). The PIP-box resides close to the 3′ end of *XCV0436* and 722 base pairs upstream of the putative *xopD* start site (Fig. 1A, top panel). A survey of PIP-boxes in Xcv 85-10 revealed that the majority of these motifs are found within 300 base pairs of the −10 promoter motif in T3S system-associated genes (Koebnik *et al*., 2006). Thus, we speculated that the actual transcriptional start site for the *xopD* gene might be closer to the PIP-box.

After further inspection of the locus, we identified a putative start codon, 78 base pairs downstream of the PIP-box (Fig. 1A,

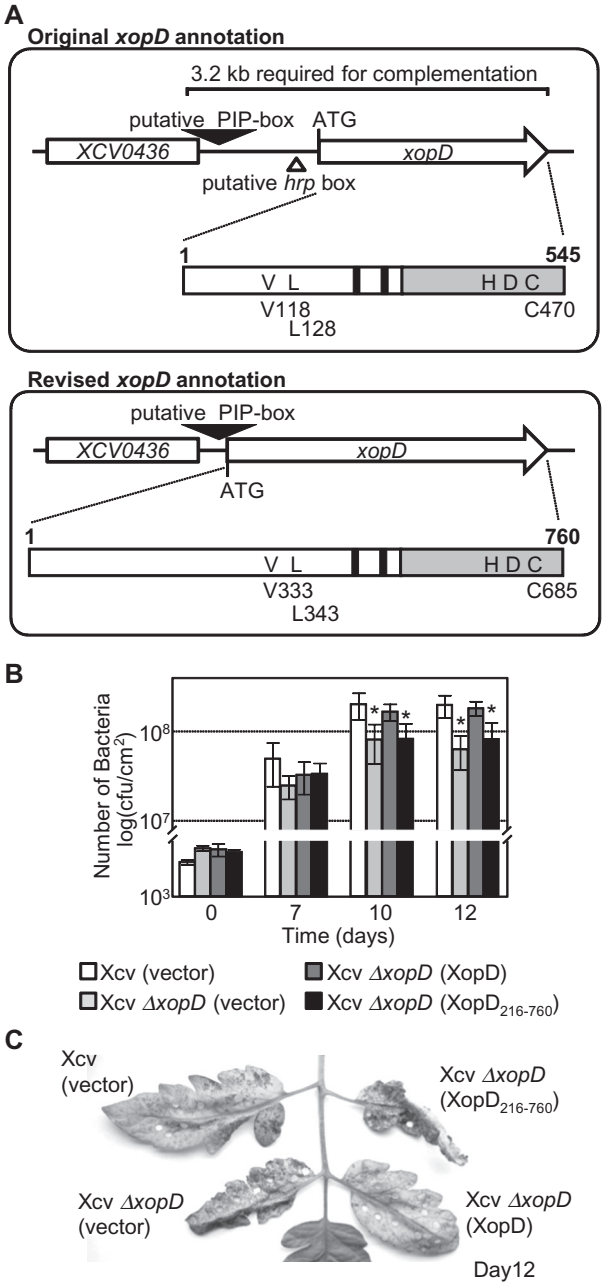

Fig. 1 Revised genome annotation and characterization of the *xopD* locus in *Xanthomonas campestris* pv. *vesicatoria* (Xcv) 85-10. (A) Original *xopD* annotation compared with the revised *xopD* annotation. Analysis of the Xcv 85-10 genome predicted the *xopD* open reading frame (ORF) to start 3′ of the putative *hrp* box (Thieme *et al*., 2005). The original *xopD* gene annotation predicted an ORF that encodes a protein of 545 amino acid residues. A 3.2-kb genomic fragment was required to complement Xcv Δ*xopD* mutant phenotypes (Kim *et al*., 2008), suggesting that this annotation might be incorrect, and an alternative *xopD* start site occurs near the putative pathogen-inducible promoter (PIP)-box. The revised *xopD* annotation shows that the ORF starts 3′ of the putative PIP-box. The *xopD* gene encodes a much larger polypeptide with a total of 760 amino acid residues. Schematic diagrams of the original and revised XopD protein coding regions are shown below the respective gene annotation arrows to compare the amino acid residues and functional domains for each predicted protein. The grey bar represents the C-terminal small ubiquitin-related modifier (SUMO) protease domain containing the catalytic core residues: histidine (H), aspartic acid (D) and cysteine (C). Black bars represent the putative ethylene-responsive element binding factor-associated amphiphilic repression (EAR) motifs. The white bar defines the N-terminal region including a DNA-binding domain. Based on the original *xopD* annotation, valine 118 (V118) and leucine 128 (L128) were shown to be required for DNA binding, and cysteine 470 (C470) for SUMO peptidase/isopeptidase activity (Hotson *et al*., 2003; Kim *et al*., 2008). Based on the revised *xopD* annotation, amino acids 1–545 in the old XopD protein sequence are equal to amino acids 216–760 in the new XopD protein sequence. Similarly, V118, L128 and C470 in the original coding sequence are equal to V333, L343 and C685, respectively, in the revised coding sequence. (B) Growth of the Xcv Δ*xopD* null mutant in tomato leaves is complemented by XopD (1–760 amino acids), but not $XopD_{216–760}$. Leaves were hand-inoculated with a 1×10^5 colony-forming units (cfu)/mL suspension of Xcv (vector) containing pVSP61 (white bar), Xcv Δ*xopD* (vector) containing pVSP61 (grey bar), Xcv Δ*xopD* (XopD) containing pVSP61(*lacZ* promoter-*xopD-His*) (dark grey bar) and Xcv Δ*xopD* ($XopD_{216–760}$) containing pVSP61(*lacZ* promoter-$xopD_{216–760}$-*His*) (black bar). Bacterial growth was quantified from 0 to 12 days post-inoculation (dpi). Data points represent mean $\log_{10}$ cfu/cm^2 ± standard deviation (SD) of three tomato plants. Error bars indicate SD. The asterisks above the bars indicate statistically significant (*t*-test, $P < 0.05$) differences between the bacterial numbers for Xcv (vector) and Xcv Δ*xopD* (vector) or Xcv Δ*xopD* ($XopD_{216–760}$). (C) Symptom development in the infected tomato leaves sampled in (B). Hole punches were used for the quantification of bacterial numbers depicted in (B). Leaves were photographed at 12 dpi. Similar phenotypes were observed in three independent experiments.

bottom panel). The *xopD* ORF defined by this ATG is predicted to encode a 760-amino-acid polypeptide (Fig. 1A, bottom panel) with a molecular weight of 85.7 kDa. This size is in better agreement with the molecular weights observed in immunoblots for XopD protein expressed in Xcv and plants (Hotson *et al*., 2003; Kim *et al*., 2008; Noël *et al*., 2002). XopD-like homologues from *Xanthomonas*, *Acidovorax* and *Pseudomonas* spp. are predicted to encode similar proteins with long N-terminal domains (Fig. 3B), consistent with this new XopD protein annotation. Furthermore, Xcv Δ*xopD* mutant phenotypes could only be complemented when a 3.2-kb DNA fragment containing the 3′ end of *XCV0436* and the *xopD* gene was used (Fig. 1A), indicating that this region contains important regulatory and functional domains defining XopD specificity. On the basis of these data, we have revised the annotation of the *xopD* locus (Fig. 1A, bottom panel) and provide functional evidence below to support these changes.

It should be noted that the XopD mature polypeptide is predicted to contain 760 amino acids (i.e. $XopD_{1–760}$), and is designated here as 'XopD'. Previously, structure–function studies (Hotson *et al*., 2003; Kim *et al*., 2008) were performed using the

C-terminal 545 amino acids of XopD based on the original annotation (Noël *et al*., 2002; Thieme *et al*., 2005). This corresponds to 216–760 amino acids in the XopD protein, and is designated here as '$XopD_{216–760}$' (see Fig. 1A).

N-terminal sequence analysis of XopD expressed in Xcv 85-10

To determine the N-terminal amino acid sequence of XopD, the entire *xopD* locus (putative promoter containing PIP-box and revised ORF) with an in-frame C-terminal 6 × His-epitope tag was cloned into the broad-host-range vector pDSK519 creating pDSK519(*xopD promoter-xopD-His*). The plasmid was conjugated into Xcv 85-10 *hrpG**, a strain that constitutively expresses T3S system-associated genes, including *xopD* (Noël *et al*., 2002), as a result of a mutation in the regulatory gene *hrpG* (Wengelnik *et al*., 1999). The Xcv 85-10 *hrpG** pDSK519(*xopD promoter-xopD-His*) strain was cultured and XopD-His protein was purified from cell extracts using Ni^{+}-affinity purification. Edman degradation protein sequence analysis revealed the XopD peptide sequence MDRIFNFDYK corresponding to the first 10 amino acids predicted by the revised annotation of the *xopD* locus (Fig. 1A, bottom panel). The first methionine in the XopD polypeptide is encoded by the ATG codon located 78 base pairs downstream of the PIP-box, validating the new annotation (Fig. 1A, bottom panel).

Construction and phenotype of a new Xcv Δ*xopD* mutant strain

Previously, we engineered a *xopD* mutant in Xcv 85-10 by homologous recombination, removing the entire *xopD* ORF predicted by the original locus annotation (Noël *et al*., 2002; Thieme *et al*., 2005). Based on our revised annotation of the *xopD* locus (Fig. 1A, bottom panel), this mutant strain still contains the 5′ region of the *xopD* ORF predicted to encode residues 1–215 of the 760-amino-acid protein. This mutant (now designated as Xcv Δ$xopD_{216–760}$) elicited a unique phenotype in susceptible VF36 tomato leaves (i.e. reduced bacterial growth and enhanced symptom development) (Kim *et al*., 2008). To confirm that these phenotypes were a result of a loss of XopD function, we deleted the entire *xopD* ORF (encoding XopD amino acids 1–760). The resulting Xcv 85-10 Δ$xopD_{1–760}$ mutant (designated throughout as Xcv Δ*xopD*) was then inoculated into susceptible VF36 tomato leaves to monitor bacterial multiplication and disease symptom production. By 12 days post-inoculation (dpi), the level of Xcv Δ*xopD* in tomato leaves was approximately three-fold less than in wild-type Xcv (Fig. 1B), whereas disease symptom production was greater in Xcv Δ*xopD*-infected leaves (Fig. 1C). Moreover, the Xcv Δ*xopD*-elicited phenotypes were similar in timing and intensity to those produced by the Xcv Δ$xopD_{216–760}$ mutant (data not shown). These data confirm that XopD plays an important role in promoting pathogen growth, whilst suppressing symptom development, and that the observed Δ*xopD* mutant phenotypes are caused by the loss of XopD function.

Complementation of Xcv Δ*xopD* mutant phenotypes in tomato

We next tested whether full-length XopD containing 760-amino-acid residues (i.e. $XopD_{1–760}$; Fig. 1A, bottom panel) could complement the Xcv Δ*xopD* mutant phenotypes in tomato. We also tested the shorter XopD protein containing the C-terminal 545-amino-acid residues (designated here as $XopD_{216–760}$) predicted by the original Xcv genome annotation (Fig. 1A, top panel). To ensure similar expression, both genes were cloned into the broad-host-range vector pVSP61 containing the *lacZ* promoter, and the resulting plasmids were conjugated into the Xcv Δ*xopD* mutant creating Xcv Δ*xopD* (XopD) and Xcv Δ*xopD* ($XopD_{216–760}$). Tomato leaves were inoculated with a 1×10^5 cells/mL suspension of bacteria, and bacterial growth and symptoms were monitored. The Xcv Δ*xopD* (XopD) strain exhibited similar phenotypes to the wild-type Xcv strain (i.e. high titres of bacteria and reduced symptom production), whereas the Xcv Δ*xopD* ($XopD_{216–760}$) strain behaved like the Xcv Δ*xopD* mutant (i.e. lower titres of bacteria and enhanced symptom production; Fig. 1B,C). XopD and $XopD_{216–760}$ proteins were equally expressed in the respective Xcv Δ*xopD* strains (Fig. S1). These data show that the entire XopD polypeptide (1–760 amino acids) is required to complement Xcv Δ*xopD* phenotypes in tomato.

XopD protein family in *Xanthomonas* spp.

Next, we examined the annotation of three *xopD-like* genes in different *Xanthomonas* species: $XopD_{XccB100}$ from Xcc strain B100; $PsvA_{Xcc8004}$ from Xcc strain 8004; $PsvA_{ATCC33913}$ from Xcc strain ATCC 33913 (Fig. 2). Based on our new *xopD* gene annotation, we identified a DNA fragment containing a PIP-box and an ATG in the $xopD_{XccB100}$ gene that was collinear with the PIP-box and start ATG in the *xopD* gene from Xcv strain 85-10 (Fig. 2). Thus, we propose that the $xopD_{XccB100}$ ORF has an alternative start site (Fig. 2) and encodes a protein containing 801 amino acids (Fig. 3). The revised annotation for the $xopD_{XccB100}$ gene was used for the phylogenetic analysis described below (Fig. 3).

Similarly, we identified an identical DNA fragment with a PIP-box and an ATG approximately 2.4 kb upstream of the $psvA_{Xcc8004}$ and $psvA_{ATCC33913}$ genes (Fig. 2). The $psvA_{Xcc8004}$ and $psvA_{ATCC33913}$ genes are 100% identical at the DNA level (Fig. 2A) and are predicted to encode proteins with short N-terminal domains uncharacteristic of other XopD-like proteins (Fig. 3B).

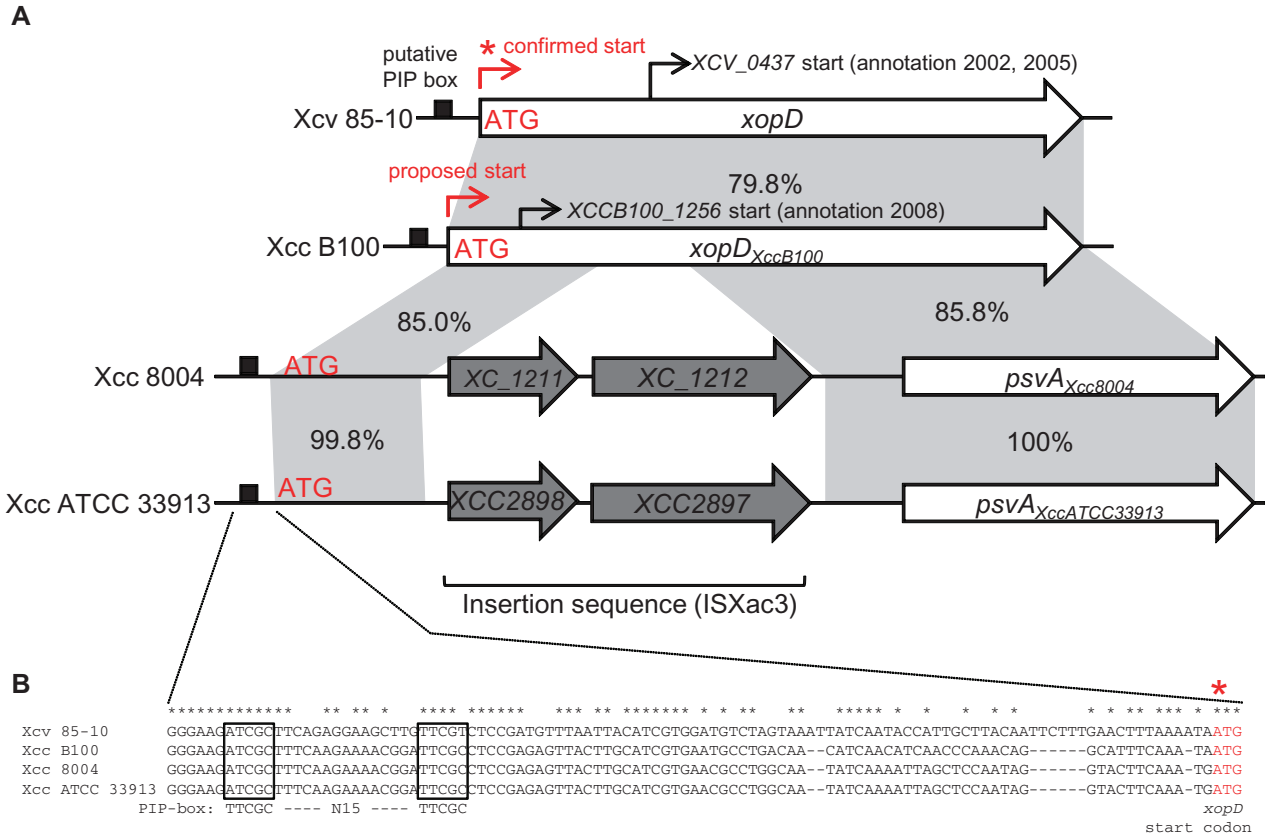

Fig. 2 Comparison of the chromosomal regions spanning the *xopD* and *xopD*-like loci in different *Xanthomonas* strains. (A) The promoter and open reading frame (ORF) for *xopD* from *Xanthomonas campestris* pv. *vesicatoria* strain 85-10 (Xcv 85-10), $xopD_{XccB100}$ from *X. campestris* pv. *campestris* strain B100 (Xcc B100), $psvA_{Xcc8004}$ from *X. campestris* pv. *campestris* strain 8004 (Xcc 8004) and $psvA_{XccATCC33913}$ from *X. campestris* pv. *campestris* strain ATCC 33913 (Xcc ATCC 33913). Black boxes, putative pathogen-inducible promoter (PIP)-boxes. Red asterisk, confirmed ATG start codon for the XopD protein. The proposed start site for $xopD_{XccB100}$ is shown at the corresponding ATG denoted in red. The original start sites annotated for *xopD* (Noël *et al*., 2002; Thieme *et al*., 2005) and $xopD_{XccB100}$ (Vorhölter *et al*., 2008) are noted by thin black arrows. The grey shading indicates identical DNA sequence shared between *xopD* and *xopD-like* genes. The percentage sequence identity is noted for the adjacent highlighted regions. The *xopD*-like loci in Xcc 8004 and Xcc ATCC 33913 are disrupted by an insertion sequence (ISXac3) containing two genes (i.e. *XC_1211* and *XC_1212* in Xcc 8004 and *XCC2898* and *XCC2897* in Xcc ATCC) resulting in a natural 5′ deletion, creating $psvA_{Xcc8004}$ and $psvA_{XccATCC33913}$, respectively. (B) Sequence alignment of the *xopD* and *xopD-like* promoter regions. Boxes indicate the putative PIP-box sequences sharing identity with the consensus motif (TTCGC—N15—TTCGC). Red asterisk indicates the confirmed ATG region in the *xopD* gene.

Genome annotation identified an insertion sequence (ISXac3) 5′ of both $psvA_{Xcc8004}$ and $psvA_{ATCC33913}$ (da Silva *et al*., 2002; Qian *et al*., 2005). Upstream of ISXac3 is a chromosomal region that contains the PIP-box and a 568-bp DNA sequence sharing 85% identity with the 5′ coding region of the $xopD_{XccB100}$ gene (Fig. 2A). Thus, the insertion sequence disrupted the coding region of $psvA_{Xcc8004}$ and $psvA_{ATCC33913}$, resulting in natural 5′ gene deletions (Fig. 2A). This explains why the $PsvA_{Xcc8004}$ and $PsvA_{ATCC33913}$ proteins are shorter than the other XopD homologues and provides a rationale as to why $PsvA_{ATCC33913}$ is not required for virulence (Castaneda *et al*., 2005). Consistent with these findings, we found that $PsvA_{Xcc8004}$ is not required for Xcc strain 8004 virulence in radish, cabbage, *Arabidopsis* and *Nicotiana benthamiana* (data not shown).

XopD protein family in phytopathogenic bacteria

We searched the National Center for Biotechnology Information (NCBI) protein database using the BLASTP program (Altschul *et al*., 1990) to find XopD homologues in the available sequenced genomes for plant pathogenic bacteria. XopD homologues were only identified in bacterial strains in the genera *Xanthomonas*, *Acidovorax* and *Pseudomonas*. A phylogenetic reconstruction of the XopD family in phytopathogenic bacteria is shown in Fig. 3A. The following proteins were used for this analysis: XopD from Xcv strain 85-10; $XopD_{XccB100}$ from Xcc strain B100; $PsvA_{Xcc8004}$ from Xcc strain 8004; $PsvA_{ATCC33913}$ from Xcc strain ATCC 33913; $XopD_{Aac}$ from *A. avenae* ssp. *citrulli* strain AAC00-1; $XopD_{Aaa}$ from *A. avenae* ssp. *avenae* strain ATCC

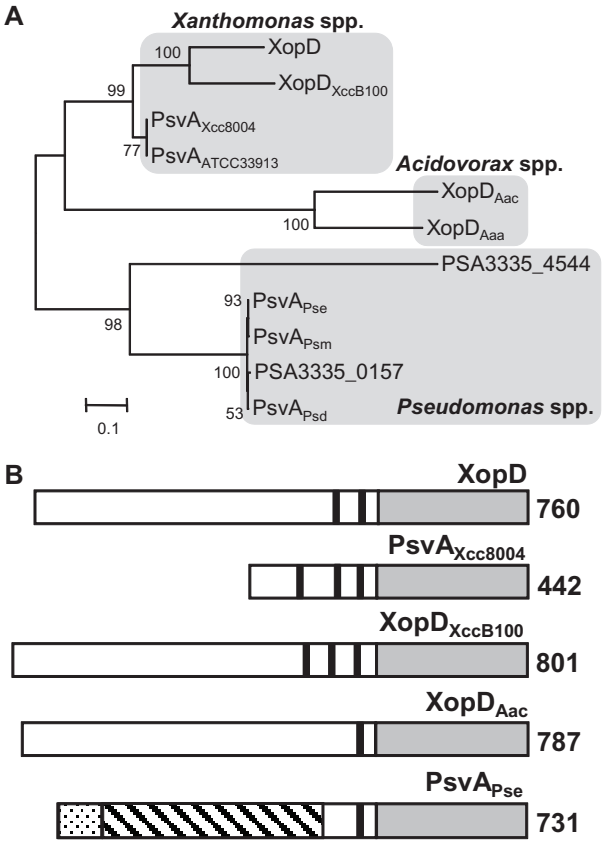

Fig. 3 XopD and XopD-like proteins of plant pathogenic bacteria. (A) Phylogenetic tree of the XopD protein family. Bootstrap values are indicated on each branch and the scale bar represents branch lengths equivalent to 0.1 amino acid changes per amino acid residue. The proteins were grouped according to genus: *Xanthomonas*, *Acidovorax* and *Pseudomonas*. XopD, XopD$_{XccB100}$, PsvA$_{Xcc8004}$, PsvA$_{ATCC33913}$, XopD$_{Aac}$, XopD$_{Aaa}$, PSA3335-4544, PsvA$_{Pse}$, PsvA$_{Psm}$, PSA3335-0157 and PsvA$_{Psd}$ proteins are from *X. campestris* pv. *vesicatoria* (Xcv) 85-10, *X. campestris* pv. *campestris* (Xcc) B100, Xcc 8004, Xcc ATCC 33913, *A. avenae* ssp. *citrulli* (Aac) AAC00-1, *A. avenae* ssp. *avenae* (Aaa) ATCC 19860, *P. savastanoi* pv. *savastanoi* NCPPB 3335, *P. syringae* pv. *eriobotryae* (Pse), *P. syringae* pv. *myricae*, *P. savastanoi* pv. *savastanoi* NCPPB 3335 and *P. syringae* pv. *dendropanacis*, respectively. (B) Domain structure of XopD and XopD-like proteins. Black bars represent putative ethylene-responsive element binding factor-associated amphiphilic repression (EAR) motifs. The grey rectangles represent C-terminal small ubiquitin-related modifier (SUMO) protease domains. For the PsvA$_{Pse}$ protein, the dotted bar represents the putative type III secretion (T3S) signal (1–97 amino acids) sharing 41% identity with AvrA1$_{PstT1.}$ The hatched bar encodes a putative DNA-binding domain (40–409 amino acids) sharing 31% identity with HsvB$_{Pab}$. The amino acid length of each protein is denoted at the C-terminal end. XopD, PsvA$_{Xcc8004}$, XopD$_{XccB100}$, XopD$_{Aac}$, XopD$_{Aaa}$ and PsvA$_{Pse}$ are from Xcv 85-10, Xcc 8004, Xcc B100, Aac AAC00-1, Aaa ATCC 19860 and Pse strains, respectively. All six proteins have the conserved catalytic core residues (His, Asp and Cys) in the SUMO protease domain. GenBank accession numbers: BK007963 (XopD), YP_242302(PsvA$_{Xcc8004}$), YP_001902662(XopD$_{XccB100}$), YP_972673(XopD$_{Aac}$), ZP_06211344(XopD$_{Aaa}$) and BAA87062(PsvA$_{Pse}$).

19860; PSA3335-4544 from *P. savastanoi* pv. *savastanoi* strain NCPPB 3335; PsvA$_{Pse}$ from *P. syringae* pv. *eriobotryae*; PsvA$_{Psm}$ from *P. syringae* pv. *myricae*; PSA3335-0157 from *P. savastanoi* pv. *savastanoi* strain NCPPB 3335; and PsvA$_{Psd}$ from *P. syringae* pv. *dendropanacis*. The closest XopD homologues cluster in a *Xanthomonas* group representing Xcv and three strains of the *Brassica* pathogen Xcc: Xcc B100, Xcc 8004 and Xcc ATCC 33913. XopD is 68.5% identical to XopD$_{XccB100}$ and 74.2% identical to PsvA$_{Xcc8004}$ and PsvA$_{ATCC33913}$. More distant homologues were found in the two *Acidovorax* spp. and five *Pseudomonas* spp. that are pathogenic to trees and shrubs (Fig. 3A).

Characteristic domains of XopD and XopD-like proteins

The most distinguishing domain of the XopD protein family is the highly conserved C-terminal SUMO protease domain (Fig. 3B). The lengths of the N-terminal domains vary significantly among members, suggesting that this region may define functional specificity (Fig. 3B). Each protein contains one to three EAR motifs ($^{L}/_{F}$DLN$^{L}/_{F}$XP) (Ohta *et al*., 2001). EAR motifs are found in plant transcription factors that often function as repressors to negatively regulate gene transcription induced during stress responses (Kazan, 2006). Both EAR motifs and SUMO protease activity are required for XopD-dependent virulence in tomato (Kim *et al*., 2008). The only homologue shown to date to be required for virulence is PsvA$_{Pse}$ from *P. syringae* pv. *eriobotryae* (Pse), the causal agent of stem canker on loquat trees (Kamiunten, 1999). The N-terminus of PsvA$_{Pse}$ contains a putative T3S signal peptide at amino acids 1–97 that is 41% identical to AvrA1 from *P. syringae* pv. *tomato* strain T1 (Almeida *et al*., 2009) and a putative DNA-binding domain, a helix-turn-helix (HTH) region, that is 30%–32% identical to HsvB and HsvG type III effectors from *Pantoea agglomerans* pv. *betae* and *Pantoea agglomerans* pv. *gypsophilae*. HsvB and HsvG are host-specificity determinants and their specific DNA-binding domain is predicted to alter host transcription during infection (Nissan *et al*., 2006). A nonspecific DNA-binding domain was identified in the XopD protein just upstream of the EAR motifs (Kim *et al*., 2008); however, its role in XopD virulence is not clear. The mutation of valine 333 (old name: V118; Fig. 1A) in the DNA-binding domain reduced XopD-dependent DNA-binding activity *in vitro* and virulence activity *in planta* (Kim *et al*., 2008). Based on the new XopD annotation, DNA-binding studies need to be repeated to determine whether the newly identified N-terminal amino acid residues impart DNA-binding specificity.

Conserved SUMO protease activity

The presence of the eukaryotic SUMO protease domain in the proteins of XopD family members brings into question how this

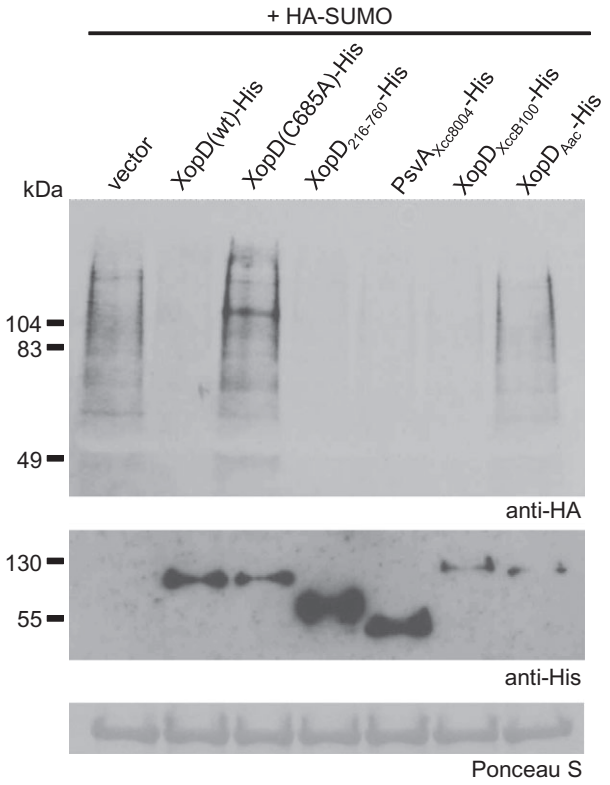

Fig. 4 Small ubiquitin-related modifier (SUMO) protease activity for XopD and XopD-like proteins. *Nicotiana benthamiana* leaves were co-infiltrated with a suspension of *A. tumefaciens* expressing tomato HA-SUMO1 with vector, XopD(wt)-His, XopD(C685A)-His, $XopD_{216–760}$-His, $PsvA_{Xcc8004}$-His, $XopD_{XccB100}$-His or $XopD_{Aac}$-His. For co-inoculations, strains were mixed equally and infiltrated into the leaf at a final density of 8×10^8 cells/mL. Sixty hours after inoculation, total protein was extracted from infected leaves and analysed by protein gel blot analysis using anti-haemagglutinin (HA) (top panel) or anti-His (bottom panel) sera, as described previously (Hotson *et al*., 2003). Ponceau S-stained ribulose-1,5-bisphosphate carboxylase/oxygenase (Rubisco) large subunit is shown as a loading control. These experiments were repeated three times with similar results.

domain is employed during different bacterial–plant interactions, and whether or not the proteins encode active enzymes. To address the latter question, we measured the SUMO isopeptidase activity for XopD members from *Xanthomonas* and *Acidovorax* spp. in an *Agrobacterium*-mediated transient expression assay in *N. benthamiana*. Haemagglutinin (HA)-SUMO and His-tagged proteins were co-expressed in *N. benthamiana* leaves for 48 h. Protein was then extracted and analysed by protein gel blot analysis to detect plant HA-SUMO–protein conjugates using HA antisera. Overexpression of HA-SUMO results in the accumulation of multiple HA-SUMO–protein conjugates (Fig. 4). Co-expression of HA-SUMO with XopD(wt)-His, but not the catalytically inactive cysteine protease XopD(C685A)-His, significantly reduced the accumulation of sumolyated proteins (Fig. 4). SUMO isopeptidase activity was observed for the truncated $XopD_{216–760}$-His protein, as expected (Hotson *et al*., 2003), and for the homologues $PsvA_{Xcc8004}$-His, $XopD_{XccB100}$-His and $XopD_{Aac}$-His. However, $XopD_{Aac}$-His was generally less stable (Fig. S3) and exhibited weaker SUMO cleavage than the other homologues (Fig. 4). XopD and all of the tested orthologues contain the conserved catalytic residues (i.e. histidine, aspartate and cysteine) found in SUMO proteases in the C48 peptidase family (see MEROPS Protease Database, http://merops.sanger.ac.uk/). However, the sequence identity of the SUMO protease domain varies. The SUMO protease domain of XopD (555–760 amino acids) is 83% identical to $XopD_{XccB100}$ (596–801 amino acids), 85.4% identical to $XopD_{Xcc8004}$ (225–442 amino acids) and 40.8% identical to $XopD_{Aac}$ (561–767 amino acids). The lower sequence identity of the SUMO protease domain of $XopD_{Aac}$ suggests that this enzyme might have alternative substrates and/or enzymatic function. Taken together, these data suggest that XopD-like proteins probably function as SUMO isopeptidases *in planta*.

Phenotype and localization of XopD family members in *N. benthamiana*

We have shown previously that the short version of XopD (i.e. $XopD_{216–760}$), based on the original annotation, elicits tissue necrosis in *N. benthamiana* leaves using *Agrobacterium*-mediated transformation assay (Kim *et al*., 2008). We noted that the necrosis phenotype correlated with the accumulation of the effector within the plant nucleus in subnuclear foci. These studies were repeated with epitope-tagged versions of full-length XopD and other family members to determine whether these phenotypes were conserved.

Overexpression of XopD in *N. benthamiana* leaves caused tissue necrosis by 6 dpi (Fig. 5A). The phenotype was similar in timing and intensity to that observed for $XopD_{216–760}$ (Fig. 5A). By contrast, overexpression of $XopD_{Aac}$ and $PsvA_{Xcc8004}$ in leaves caused chlorosis, but no visible tissue necrosis (Fig. 5A). $XopD_{XccB100}$ overexpression elicited some tissue collapse; however, symptom development was slower than that observed for XopD and $XopD_{216–760}$ (Fig. 5A).

To monitor effector localization in *N. benthamiana* leaves, the proteins were tagged at the N-termini with yellow fluorescent protein (YFP). YFP-XopD was localized to the plant nucleus and accumulated in subnuclear foci, as observed for the shorter version YFP-$XopD_{216–760}$ (Fig. 5B). However, YFP-XopD did not accumulate to the same levels as YFP-$XopD_{216–760}$, suggesting that it may be less stable (Fig. 5B, Fig. S3). YFP-$XopD_{XccB100}$ localization and protein abundance were similar to those of YFP-XopD (Fig. 3B, Fig. S3). By contrast, YFP-$PsvA_{Xcc8004}$ was localized to the plant cytoplasm and diffusely throughout the nucleus, exhibiting a similar localization pattern to YFP alone (Fig. 5B).

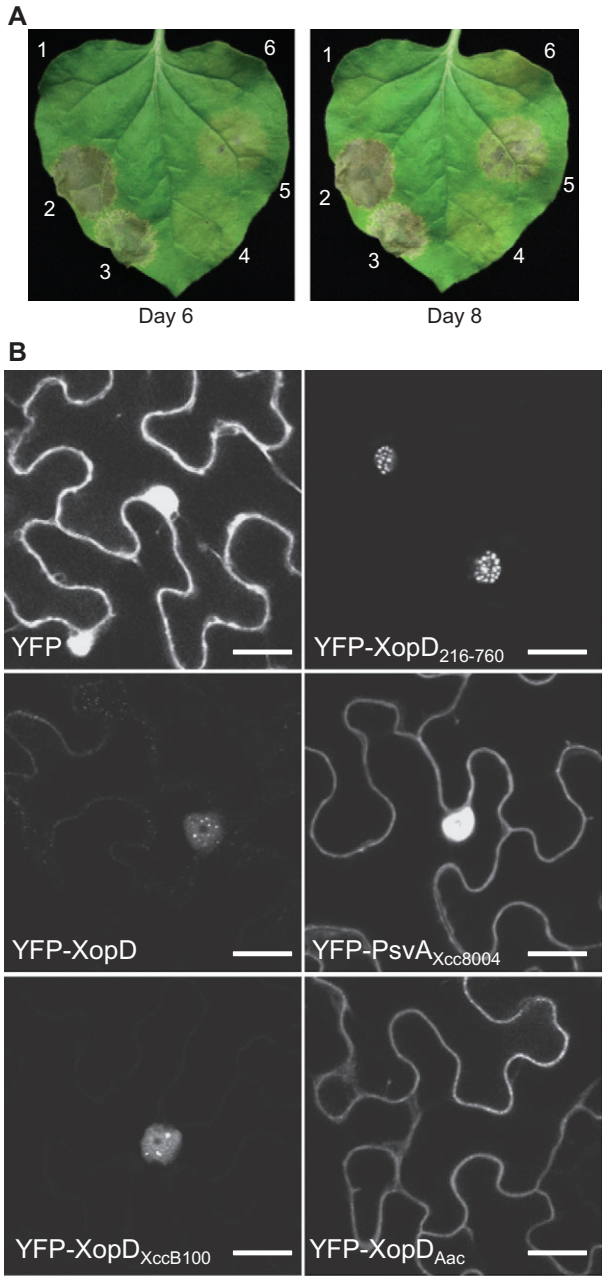

Fig. 5 Phenotypes of *Agrobacterium*-mediated transient expression of XopD and XopD-like proteins in *Nicotiana benthamiana*. (A) Necrosis phenotype in *N. benthamiana* leaves. Leaves were infiltrated with a 6 × 10^8 cells/mL suspension of *Agrobacterium tumefaciens* expressing the following: 1, vector control; 2, XopD; 3, $XopD_{216–760}$; 4, $PsvA_{Xcc8004}$; 5, $XopD_{XccB100}$; 6, $XopD_{Aac}$. All proteins were tagged with the 6 × His epitope at the C-terminus. The leaves were photographed at 6 and 8 days post-inoculation (dpi). Protein expression was confirmed by protein gel blot analysis (Fig. S2). (B) Subcellular localization of XopD and XopD-like proteins in *N. benthamiana*. Leaves were infiltrated with a 6 × 10^8 cells/mL suspension of *Agrobacterium tumefaciens* expressing yellow fluorescent protein (YFP), YFP-$XopD_{216–760}$, YFP-XopD, YFP-$PsvA_{Xcc8004}$, YFP-$XopD_{XccB100}$ or YFP-$XopD_{Aac}$. At 60 h post-inoculation, leaf epidermal cells were visualized by confocal microscopy at × 63. Scale bar, 20 μm. Protein expression was confirmed by protein gel blot analysis (Fig. S4). The experiments were repeated three times with similar results.

This suggests that $PsvA_{Xcc8004}$ and XopD might be targeted to different subcellular sites. Alternatively, the YFP-$PsvA_{Xcc8004}$ localization pattern might simply reflect the localization of a degraded form of YFP-$PsvA_{Xcc8004}$ under the conditions tested. Interestingly, YFP-$XopD_{Aac}$ was excluded from the plant nucleus and localized to the cytoplasm and possibly plasma membrane (Fig. 5B). Taken together, these data suggest that XopD and XopD-like proteins are targeted to distinct sites within plant cells. Furthermore, they indicate that the localization of this class of effector to subnuclear foci correlates with leaf tissue necrosis in *N. benthamiana*.

XopD-like effectors do not complement the Xcv Δ*xopD* mutant

We next examined whether the XopD-like effectors (i.e. $XopD_{XccB100}$, $PsvA_{Xcc8004}$ and $XopD_{Aac}$) could complement the Xcv Δ*xopD* mutant phenotype in infected tomato leaves. None of the effectors restored Xcv Δ*xopD* growth to wild-type Xcv levels in infected tomato leaves or suppressed the onset of symptom development at 12 dpi (Fig. 6). This indicates that SUMO protease activity alone, which is shared by all of the XopD-like proteins, is not sufficient to suppress the Δ*xopD* mutant phenotype.

Amino acids 1–379 of XopD control its virulence function

The strong identity (68.1%) between XopD and $XopD_{XccB100}$ led us to investigate whether or not these effectors elicit similar host phenotypes and, possibly, virulence function. First, we asked whether $XopD_{XccB100}$ is required for Xcc B100 growth and symptom production in infected radish, *A. thaliana* and *N. benthamiana* leaves. Deletion of the $xopD_{XccB100}$ gene from the Xcc B100 genome did not affect the length of disease lesions in infected radish leaves or bacterial multiplication in *A. thaliana* and *N. benthamiana* leaves (Fig. S4). Thus, under the conditions tested, $XopD_{XccB100}$ is not required for Xcc B100 virulence in these hosts.

Next, we compared XopD and $XopD_{XccB100}$ protein sequences to determine whether we could identify key amino acids or motifs that might impart effector specificity. The N-terminal domains share 64.1% identity and the C-terminal domains share 82.1% identity (Fig. S5). Two regions were notably different between XopD and $XopD_{XccB100}$: one in the N-terminal domain and one in the junction between the N-terminal domain and the EAR motifs (Fig. S5). To determine whether either region is required for XopD specificity, we created two chimeric fusion

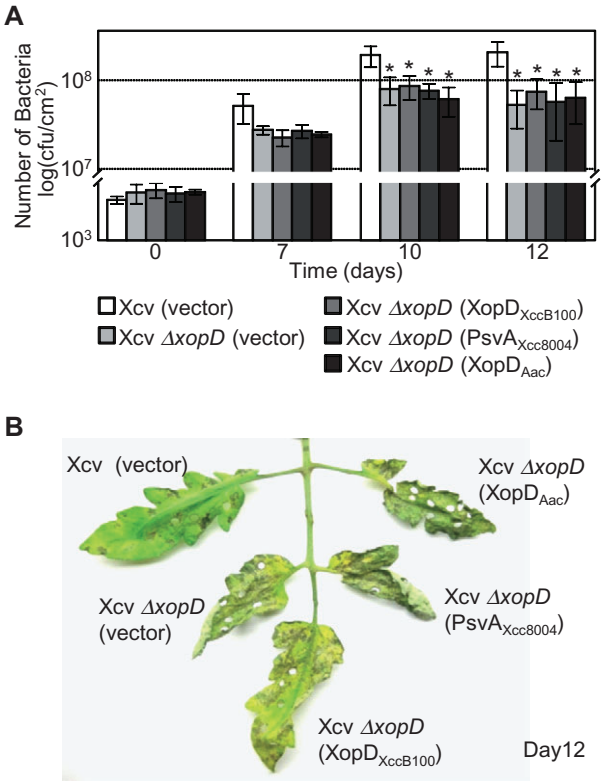

Fig. 6 $XopD_{XccB100}$, $PsvA_{Xcc8004}$ and $XopD_{Aac}$ cannot complement *Xanthomonas campestris* pv. *vesicatoria* (Xcv) Δ*xopD* mutant phenotypes in tomato leaves. (A) Growth of Xcv strains in tomato leaves. Leaves were hand-inoculated with a 1×10^5 cells/mL suspension of Xcv (vector) containing pVSP61 (white bar), Xcv Δ*xopD* (vector) containing pVSP61 (light grey bar), Xcv Δ*xopD* ($XopD_{XccB100}$) containing pVSP61(*lacZ* promoter-*$XopD_{XccB100}$-His*) (grey bar), Xcv Δ*xopD* ($PsvA_{Xcc8004}$) containing pVSP61(*lacZ* promoter-*$PsvA_{Xcc8004}$-His*) (dark grey bar) or Xcv Δ*xopD* ($XopD_{Aac}$) containing pVSP61(*lacZ* promoter-*$xopD_{Aac}$-His*) (black bar). Bacterial growth was quantified from 0 to 12 days post-inoculation (dpi). Data points represent mean $\log_{10}$ colony-forming units (cfu)/cm^2 ± standard deviation (SD) of three tomato plants. Error bars indicate SD. The asterisks above the bars indicate statistically significant (*t*-test, $P < 0.05$) differences between the bacterial numbers for Xcv (vector) and Xcv Δ*xopD* (vector) or Xcv Δ*xopD* expressing $XopD_{XccB100}$, $PsvA_{Xcc8004}$ or $XopD_{Aac}$. (B) Phenotype of Xcv-infected tomato leaves sampled in (A). Hole punches were used for the quantification of the bacterial numbers depicted in (A). Leaves were photographed at 12 dpi. Similar phenotypes were observed in three independent experiments.

proteins, XopDvc1 and XopDvc2. XopDvc1 contains the N-terminal domain (amino acids 1–457) of XopD fused to the third EAR motif and SUMO protease domain of $XopD_{XccB100}$ (amino acids 533–801) (Fig. 7A). XopDvc2 contains the N-terminal domain (amino acids 1–379) of XopD fused to the C-terminal half of $XopD_{XccB100}$ (amino acids 399–801) containing the junction region, three EAR motifs and the SUMO protease domain (Fig. 7A). Xcv Δ*xopD* strains expressing XopDvc1 or XopDvc2 were able to restore bacterial growth in tomato leaves to wild-type Xcv levels (Fig. 7B) and suppress the onset of tissue necrosis (Fig. 7C). These data show that the N-terminal 379 amino acids of XopD are required for XopD-dependent virulence phenotypes in tomato. Furthermore, only one EAR motif is required to complement the Δ*xopD* mutant phenotype (Fig. 7), consistent with previous structure–function studies showing that XopD's EAR motifs are functionally redundant (Kim *et al*., 2008). Interestingly, the N-terminal region of $XopD_{XccB100}$ contains a 14-amino-acid peptide that does not exist in XopD (Fig. S5). It remains to be determined which amino acid(s) in the N-terminal 379 amino acids of XopD define specificity.

DISCUSSION

Comparative analysis of the XopD effector family in phytopathogenic bacteria revealed that XopD-like proteins are restricted to species within the three genera of Proteobacteria—*Xanthomonas*, *Acidovorax* and *Pseudomonas* (Fig. 3A). All XopD effector family members contain EAR motif(s) and a conserved C-terminal SUMO protease domain (Fig. 3B). The family members, however, differ in the sequence and length of their N-terminal domains (Figs 2A,3B). This suggests that the N-terminal domain of XopD and XopD-like effectors might impart substrate and/or host specificity. It also suggests that the original annotation of the *xopD* locus might be incorrect, considering that the XopD protein was predicted to have only 545 amino acids (Noël *et al*., 2002; Thieme *et al*., 2005), a size significantly smaller than $XopD_{Aac}$ (787 amino acids) from *A. avenae* ssp. *citrulli* strain AAC00-1.

Given these assumptions, we carefully inspected the intergenic region of the Xcv 85-10 genome between the *XCV0436* locus and the *xopD* locus for an alternative promoter and start site. We identified a putative PIP-box and ATG just downstream of the adjacent *XCV0436* locus (Fig. 1A). Using this ATG as the putative start codon, the respective *xopD* ORF predicts a protein with 760 amino acids (Fig. 1A) with a longer N-terminal domain sharing strong similarity with $XopD_{Aac}$ (Fig. 3). N-terminal sequence analysis of the purified XopD-His protein isolated from Xcv 85-10 cell extracts confirmed that this ATG encodes the first methionine of the mature XopD protein. We therefore revised the annotation of the *xopD* locus in Xcv 85-10 (Fig. 1A).

Using the new *xopD* annotation, we analysed all of the *xopD-like* genes from *Xanthomonas* spp. We propose that the annotation of the *$xopD_{XccB100}$* gene from Xcc B100 should be revised. We identified a PIP-box and an alternative start site in the *$xopD_{XccB100}$* gene that is collinear with the respective region in the *xopD* gene (Fig. 2A). The putative $XopD_{XccB100}$ protein is predicted to have 801 amino acids, sharing strong similarity with both XopD and $XopD_{Aac}$ (Fig. 3). By contrast, it was unclear why two smaller XopD-like proteins with short N-terminal domains

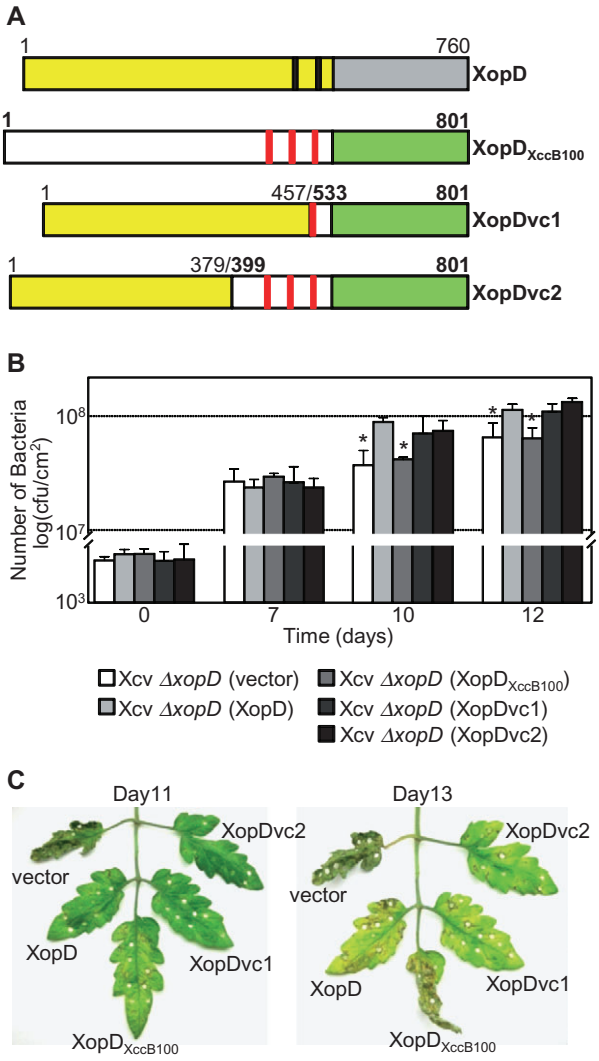

Fig. 7 Chimeric XopD-XopD$_{XccB100}$ fusion proteins complemented *Xanthomonas campestris* pv. *vesicatoria* (Xcv) Δ*xopD* mutant phenotypes in infected tomato leaves. (A) Schematic diagram of wild-type XopD (1–760 amino acids) and XopD$_{XccB100}$ (1–801 amino acids) and two chimeric fusion proteins, XopDvc1 and XopDvc2. XopDvc1 contains amino acids 1–457 of XopD fused to amino acids 533–801 of XopD$_{XccB100}$. XopDvc2 contains amino acids 1–379 of XopD fused to amino aids 399–801 of XopD$_{XccB100}$. The yellow rectangles represent XopD's N-terminal domain before its small ubiquitin-related modifier (SUMO) protease domain (grey rectangle), and the black bars represent the putative ethylene-responsive element binding factor-associated amphiphilic repression (EAR) motifs. The white rectangles represent XopD$_{XccB100}$'s N-terminal domain before its SUMO protease domain (green rectangle) and the red bars represent putative EAR motifs. (B) Growth of Xcv strains in tomato leaves. Leaves were hand-inoculated with a 1×10^5 cells/mL suspension of Xcv Δ*xopD* (vector) containing pVSP61 (white bar), Xcv Δ*xopD* (XopD) containing pVSP61(*lacZ* promoter-*XopD-His*) (light grey bar), Xcv Δ*xopD* (XopD$_{XccB100}$) containing pVSP61(*lacZ* promoter-*XopD$_{XccB100}$-His*) (grey bar), Xcv Δ*xopD* (XopDvc1) containing pVSP61(*lacZ* promoter-*XopDvc1-His*) (dark grey bar) or Xcv Δ*xopD* (XopDvc2) containing pVSP61(*lacZ* promoter-*XopDvc2-His*) (black bar). Data points represent mean $\log_{10}$ colony-forming units (cfu)/cm^2 ± standard deviation (SD) of three tomato plants. Error bars indicate SD. The asterisks above the bars indicate statistically significant (*t*-test, $P < 0.05$) differences between the bacterial numbers for Xcv (XopD) and Xcv Δ*xopD* (vector) or Xcv Δ*xopD* (XopD$_{XccB100}$). (C) Phenotype of the Xcv-infected tomato leaves sampled in (B). Hole punches were used for the quantification of the bacterial numbers depicted in (B). Leaves were photographed at 11 and 13 days post-inoculation. Similar phenotypes were observed in three independent experiments.

existed in the Xcc 8004 and Xcc ATCC 33913 genomes (i.e. PsvA$_{Xcc8004}$ and PsvA$_{XccATCC33913}$, respectively). After further inspection of these loci, we identified an insertion sequence element in the 5′ coding region of the respective ORFs that disrupts a potentially long ORF (Fig. 2). It is not known whether *psvA$_{Xcc8004}$* and *psvA$_{XccATCC33913}$* are expressed or produce truncated protein in these Xcc strains. Neither *psvA$_{Xcc8004}$* (J.-G. Kim and M. B. Mudgett, data not shown) nor *psvA$_{XccATCC33913}$* (Castaneda *et al*., 2005) are required for Xcc virulence in their host plants. Intriguingly, XopD$_{XccB100}$, despite its strong sequence similarity with XopD, was not required for Xcc B100 virulence in *Arabidopsis*, *N. benthamiana* and radish (Fig. S4). Taken together, these data suggest that XopD-like effectors are not important for Xcc–plant interactions.

In *Pseudomonas* spp., *xopD-like* genes were only identified in strains that cause bacterial canker or gall disease on trees and shrubs. For example, *xopD-like* ORFs encoding PsvA$_{Pse}$, PsvA$_{Psm}$ and PsvA$_{Psd}$ are present in *P. syringae* pv. *eriobotryae* which causes stem canker on loquat trees, *P. syringae pv. myricae* which causes bacterial gall on Chinese bayberry and *P. syringae pv. dendropanacis* which causes bacterial gall of *Dendropanax*, respectively. Interestingly, *P. savastanoi* pv. *savastanoi* strain NCPPB 3335, the causal agent of olive knot (or gall) disease on olive, has two closely related *xopD-like* ORFs (PSA3335-4544 and PSA3335-0157) (Fig. 3).

Of the XopD-like proteins in *Pseudomonas* spp., only PsvA$_{Pse}$ is a known virulence factor that is required for both bacterial multiplication and canker development on loquat trees (Kamiunten, 1999). The N-terminal domain of PsvA$_{Pse}$ following the putative T3S signal shares approximately 30% protein identity with the putative DNA-binding domain of two host specificity determinants, HsvB and HsvG, from *P. agglomerans* pv. *betae* and *P. agglomerans* pv. *gypsophilae*, which induce galls on beet and/or gypsophila (Nissan *et al*., 2006). HsvB and HsvG do not have SUMO protease domains; however, they are known to localize to the plant nucleus and to specifically bind double-stranded DNA (Nissan *et al*., 2006). It is not known whether PsvA$_{Pse}$ localizes to the plant nucleus and binds DNA. Whether or not XopD-like proteins in *Pseudomonas* spp. play a role in the initiation and/or development of galls and tumours remains to be determined.

Importantly, the new *xopD* gene annotation has resolved two unexplained issues that emerged during the course of our work. First, we could not complement an Xcv Δ*xopD*$_{216–760}$ mutant (previously referred to as the 'Xcv Δ*xopD* mutant') with a short genomic fragment encoding XopD$_{216–760}$ (Kim *et al*., 2008). Complementation of the Xcv Δ*xopD*$_{216–760}$ mutant only occurred when a 3.2-kb DNA fragment spanning the 3′ region of the *XCV0436* gene and the 3′ end of the *xopD* gene (Kim *et al*., 2008) was used, because it contained the entire *xopD*$_{1–760}$ ORF (Fig. 1A). In this work, we have shown that a construct containing *xopD*$_{1–760}$ is sufficient to complement the mutant phenotypes (i.e. reduced pathogen growth and increased symptom development) caused by an Xcv Δ*xopD* null mutant (Fig. 1B,C). Second, we could not explain why XopD protein isolated from Xcv always migrated as a much larger polypeptide than expected in protein gels (Kim *et al*., 2008; Noël *et al*., 2002). The original annotation predicted the protein to be 61.3 kDa (Noël *et al*., 2002). The revised annotation predicts XopD to encode an 85.7-kDa protein.

Our new annotation of the *xopD* locus, however, questions whether or not the XopD type III translocation data are still valid. Previously, we used the adenylate cyclase (Cya) reporter assay to demonstrate that XopD was translocated into the plant cell in a type III-dependent manner (Hotson *et al*., 2003). These data are still valid because the construct used for the analysis [i.e. pVSP61(P-*xopD-cya*)] contained the *xopD* promoter region with the PIP-box and the entire *xopD* ORF which encodes the XopD mature polypeptide, 1–760 amino acids.

We still do not know how XopD enters the plant nucleus once it is translocated into the plant cell. No obvious nuclear localization signals were identified by structure–function analysis (J.-G. Kim and M. B. Mudgett, unpublished data). However, it is clear that amino acids 216–499 of XopD are sufficient for trafficking EYFP to subnuclear foci (Hotson *et al*., 2003). We speculate that XopD-interacting partners may translocate and/or stabilize the effector to subnuclear foci. The absence of the N-terminal domain in PsvA$_{Xcc8004}$ as a result of mutation (Fig. 2) may explain why it is not trafficked to subnuclear foci (Fig. 5B). Alternatively, the diffuse nuclear localization pattern of PsvA$_{Xcc8004}$ might simply reflect the subcellular distribution of a smaller YFP-PsvA$_{Xcc8004}$ degradation product (i.e. YFP). The exclusion of YFP-XopD$_{Aac}$ from the plant nucleus (Fig. 5B) suggests that this XopD-like effector does not associate with nuclear-associated proteins and/or interacts with different host targets. Interestingly, XopD$_{Aac}$ exhibited the weakest SUMO isopeptidase activity of all the XopD-like proteins assayed (Fig. 4). XopD$_{Aac}$ may be a less efficient enzyme. Or, it may not have access to the major pool of sumoylated proteins in the plant nucleus. These data suggest that the XopD effector family may target distinct host substrates in different subcellular compartments within plant cells.

One of our long-term goals is to find XopD substrates that regulate defence responses and disease symptom development in tomato. We have performed several protein interaction studies with the shorter version of the XopD protein and were unable to isolate nuclear proteins that specifically interact with XopD. Knowing that the XopD effectors are generally quite similar, except for their long N-terminal domains, prompted us to determine whether the N-terminus of XopD controls host specificity and, possibly, substrate specificity. By performing domain swap experiments between XopD and XopD$_{XccB100}$, the closest orthologue in *Xanthomonas* spp., we showed that the N-terminus of XopD is required for XopD-specific phenotypes in tomato (i.e. maximal Xcv growth and suppression of defence responses and disease symptom development) (Fig. 7). Proteins containing amino acids 1–379 of XopD fused to the EAR motifs and SUMO protease domain from XopD$_{XccB100}$ complemented Xcv Δ*xopD* mutant phenotypes in tomato leaves (Fig. 7). Thus, the N-terminus of XopD defines host specificity, whereas the EAR motifs and SUMO protease domain of XopD and XopD$_{XccB100}$ appear to be functionally redundant. The identification of tomato proteins that specifically interact with the N-terminal domain of XopD should reveal new insight into the mechanism(s) by which this effector modulates signalling in the Xcv–tomato interaction.

EXPERIMENTAL PROCEDURES

Bacterial strains and growth conditions

Xcv strain 85-10, Xcc strain B100 (obtained from Alfred Pühler, Universität Bielefeld, Bielefeld) and *A. avenae* ssp. *citrulli* strain AAC00-1 (obtained from David A. Stahl, University of Washington, Seattle) were grown on nutrient yeast glycerol agar (NYGA) (Turner *et al*., 1984), tryptone yeast (TY) agar (Aguilar *et al*., 1985) and yeast extract–dextrose–$CaCO_3$ (YDC) agar (Jones *et al*., 2001), respectively, at 28 °C. *Escherichia coli* DH5α and *Agrobacterium tumefaciens* C58C1 (pCH32) were grown on Luria agar medium (Sambrook *et al*., 1989) at 37 and 28 °C, respectively. Antibiotics were used in *E. coli* cultures at 100 μg/mL for carbenicillin, 50 μg/mL for kanamycin, 50 μg/mL for spectinomycin and 10 μg/mL for tetracycline, and in *Agrobacterium tumefaciens* cultures at 100 μg/mL for rifampicin, 35 μg/mL for kanamycin and 5 μg/mL for tetracycline, and in Xcv strain 85-10 cultures at 100 μg/mL for rifampicin, 50 μg/mL for kanamycin, 50 μg/mL for spectinomycin and 10 μg/mL for tetracycline, and in Xcc strain B100 cultures at 800 μg/mL for streptomycin and 30 μg/mL for gentamycin.

XopD purification and N-terminal sequence analysis

To determine the N-terminal amino acid sequence of the XopD protein from Xcv strain 85-10, Xcv 85-10 *hrpG** containing pDSK519(0.9-kb *xopD promoter-xopD-6xHis*) was grown in

NYGB medium for 16 h, and then subcultured in 2 L of NYGB medium for 12 h. Cells were harvested and lysed in lysis buffer [100 mM NaH_2PO_4, 10 mM tris(hydroxymethyl)aminomethane (Tris), 8 M urea, pH 8.0]. Cellular debris was removed by centrifugation at 14 000 ***g*** for 30 min. The supernatant was incubated with nickel-nitrilotriacetic acid Superflow resin (Qiagen, Valencia, CA, USA) for 1 h at room temperature and then loaded into a column. The resin was washed with wash buffer (100 mM NaH_2PO_4, 10 mM Tris, 8 M urea, pH 6.3) twice. His-tagged XopD protein was eluted with elution buffer (100 mM NaH_2PO_4, 10 mM Tris, 8 M urea, pH 4.5) and the eluate was concentrated using a Microcon filter unit with an Ultracel YM-30 membrane (Millipore, Billerica, MA, USA), according to the manufacturer's instructions. Purified proteins were separated by 6% sodium dodecylsulphate-polyacrylamide gel electrophoresis (SDS-PAGE), transferred onto a Sequi-Blot poly(vinylidene difluoride) (PVDF) membrane (Bio-Rad, Hercules, CA, USA) and then stained with Ponceau S. For N-terminal sequence analysis, the XopD-His band was excised from the membrane and submitted to the Stanford Protein and Nucleic Acid Facility for Edman protein sequence analysis.

Construction of Xcv Δ*xopD* and Xcc B100 Δ$xopD_{XccB100}$ null mutants

Standard methods were used for DNA cloning, restriction mapping and gel electrophoresis (Sambrook *et al*., 1989). To construct a new Xcv 85-10 *xopD* deletion mutant based on the revised annotation for the locus, the 0.9-kb upstream and 1.2-kb downstream regions of the *xopD* gene were PCR amplified using Xcv 85-10 genomic DNA as template and cloned into pENTR/D-TOPO (Invitrogen, Carlsbad, CA, USA) (primer sets: for upstream, 5′-GGTCTAGAAGCTGCGCACCGG-3′ and 5′-GGATCCTATTTTAAAGTTCAAAGAATTGTAAGC-3′; for downstream, 5′-GGATCCTAGCAGTTCGACCATCAGC-3′ and 5′-CGGGCGAATTCCGC-3′). The spectinomycin resistant gene cassette was cloned into the *Bam*HI site between the upstream and downstream regions of *xopD* in pENTR/D-TOPO and the resulting 3.6-kb insert was recombined into the suicide vector pLVC18-Rfc (obtained from Brian Staskawicz, University of California, Berkeley) using the Gateway system. The final plasmid [pLVC18(*xopD-Sp-xopD*)] was introduced into Xcv 85-10 by triparental mating. Xcv transconjugants (Rif^r, Sp^r, Tet^s) were then selected and analysed by PCR to confirm that homologous recombination occurred at the *xopD* locus. The same strategy was used to engineer the Xcc B100 $xopD_{XccB100}$ deletion mutant. Briefly, the 0.9-kb upstream and 1.2-kb downstream regions of $xopD_{XccB100}$ were PCR amplified using Xcc B100 genomic DNA as template (primer sets: for upstream, 5′-CACCGATACATTGACCGAAACA-3′ and 5′-GGGATCCTATTTGAAATGCCTGTTTGGGT-3′; for downstream, 5′-GGGATCCTTCGACCATCGGCGGTAG-3′ and 5′-GGGCGCGCCAGGGCCATTCGGC-3′). For antibiotic selection of the deletion mutant, a gentamycin resistant gene cassette was used to ultimately create pLVC18($xopD_{XccB100}$-*Gm*-$xopD_{XccB100}$). Finally, Xcc transconjugants (Rif^r, Gm^r, Tet^s) were then selected and analysed by PCR to confirm that homologous recombination occurred at the $xopD_{XccB100}$ locus.

Phylogenetic tree construction

To construct a phylogenetic tree of XopD and XopD-like proteins, the Xcv 85-10 XopD amino acid sequence was queried against the nr database in GenBank using the BLASTP program. Protein sequences from plant pathogenic bacteria and full-length hits with an *E*-value of less than 10^{-10} were included for construction. The retrieved amino acid sequences were aligned using the CLUSTALX 2.0 program (Thompson *et al*., 1997). From the aligned data, the phylogenetic tree (with 1000 bootstrap replicates) was constructed by the neighbour-joining method in the MEGA4 program (Tamura *et al*., 2007) using a Poisson correction substitution model and including sites with a pairwise deletion of gaps/missing data.

Constructs for transient protein expression in *N. benthamiana*

For transient expression of XopD and XopD-like proteins in *N. benthamiana*, $xopD_{1–760}$, $xopD_{216–760}$, $psvA_{Xcc8004}$, $xopD_{XccB100}$ and $xopD_{Aac}$ were PCR amplified using genomic DNA as template (primer sets: for $xopD_{1–760}$, 5′-GGAGATCTCCATGGACAGGATATTTAATTTCG-3′ and 5′-GGTCTAGACTAATGATGATGATGATGATGGAACTTTTTCCACCACTTGCTTTTC-3′; for $xopD_{216–760}$, 5′-GGGGATCCCCATGACCCCAGATCAGAAG-3′ and 5′-GGTCTAGACTAATGATGATGATGATGATGGAACTTTTTCCACCACTTGCTTTTC-3′; for $psvA_{Xcc8004}$, 5′-GGATCCCCATGGAATCCCAAGACCCG-3′ and 5′-GGTCTAGACTAATGATGATGATGATGATGGAACTTTTTCCACCACTTGC-3′; for $xopD_{XccB100}$, 5′-GGGATCCCCATGGACAGATTATTTAATTTTGACTATAAA-3′ and 5′-GGTCTAGATTAGTGATGATGATGATGATGCTGGAACTTCCACCACTTGCTTT-3′; and for $xopD_{Aac}$, 5′-GGGATCCCCATGGATAACTTTTTCAACTTCGATAT-3′ and 5′-GGTCTAGACTAGTGATGATGATGATGATGGAACTTCCACCATTTCTTGTTTTTC-3′). It should be noted that the numbering scheme for $xopD_{1–760}$ and $xopD_{216–760}$ refers to the amino acids in the newly annotated Xcv 85-10 XopD protein which is predicted to encode 760 amino acids. The respective PCR products were cloned into pCRII, generating pCRII($xopD_{1–760}$-*His*, $xopD_{216–760}$-*His*, $psvA_{Xcc8004}$-*His*, $xopD_{XccB100}$-*His* or $xopD_{Aac}$-*His*) and sequenced. The *Bam*HI- or *Bgl*II-*Xba*I fragment for each construct was subcloned into the pEZRK-LCY plasmid with or without an N-terminal YFP fusion.

Constructs for Xcv Δ*xopD* complementation analysis

To test whether XopD and XopD-like proteins can complement the Xcv Δ*xopD* mutant phenotype, two Xcv 85-10 *xopD* genes

(*xopD*$_{1–760}$ and *xopD*$_{216–760}$) and three *xopD*-like genes (*psvA*$_{Xcc8004}$, *xopD*$_{XccB100}$ and *xopD*$_{Aac}$) were PCR amplified and cloned under the *lacZ* promoter in the broad-host-range vector pVSP61. To generate an *Nco*I site at the 3′ end of the *lacZ* promoter in pBSII, the plasmid was PCR amplified using the primer set (5′-GGCATGCCATGGCTGTTTCCTGTGTGAAATTG-3′ and 5′-GGCAT GCCATGGTTACGCCAAGCGCGC-3′), and the PCR product was digested with *Nco*I and self-ligated, generating pBSN. Partial *Nco*I-*Xba*I fragments from pCRII(*xopD*$_{1–760}$-*His*, *xopD*$_{216–760}$-*His*, *psvA*$_{Xcc8004}$-*His*, *xopD*$_{XccB100}$-*His* or *xopD*$_{Aac}$-*His*) were subcloned into the *Nco*I site of pBSN, and the resulting *Pvu*II fragments from the respective plasmids were subcloned into pVSP61, generating pVSP61(*lacZ* promoter-*xopD*$_{1–760}$-*His*), pVSP61(*lacZ* promoter-*xopD*$_{216–760}$-*His*), pVSP61(*lacZ* promoter-*psvA*$_{Xcc8004}$-*His*), pVSP61(*lacZ* promoter-*xopD*$_{XccB100}$-*His*) and pVSP61(*lacZ* promoter-*xopD*$_{Aac}$-*His*).

Agrobacterium-mediated transient protein expression in *N. benthamiana*

Agrobacterium tumefaciens strain C58C1 (pCH32) (Tai *et al*., 1999) was used for transient protein expression *in planta*. Strains were grown overnight at 28 °C on Luria agar medium containing 100 μg/mL rifampicin, 5 μg/mL tetracycline and 35 μg/mL kanamycin. Bacteria were incubated in induction medium [10 mM 2-(*N*-morpholino)ethanesulphonic acid (MES), pH 5.6, 10 mM $MgCl_2$ and 150 mM acetosyringone; Acros Organics, Geel, Belgium] for 2 h before inoculation. *Nicotiana benthamiana* leaves were hand-inoculated with a single bacterial suspension [6×10^8 colony-forming units (cfu)/mL] or two bacterial suspensions (8×10^8 cfu/mL) in induction medium. Plants were incubated at room temperature under continuous low light for 2–4 days.

SUMO protease assay

SUMO protease activity was monitored as described by Hotson *et al*. (2003). XopD or candidate enzymes were transiently co-expressed in *N. benthamiana* with tomato HA-SUMO1 using the *Agrobacterium* expression assay. Genes encoding the enzymes were cloned into pMDD1 and tomato HA-SUMO1 was cloned into pATC940 (Hotson *et al*., 2003). Sixty hours after inoculation, leaves were collected and frozen. Protein was extracted and analysed as described below.

Microscopy

Agrobacterium tumefaciens-infected *N. benthamiana* leaves were analysed approximately 48–60 h after inoculation. Leaf discs were placed on a slide and visualized using a × 63 water immersion objective lens (numerical aperture 1.2) on a Leica TCS SP5 confocal microscope (Leica Microsystems Inc., Bannockburn, IL, USA) with Leica LAS AF software. YFP was excited at 514 nm by an argon laser and emitted light was captured at 520–565 nm.

Construction of Xcv 85-10 XopD and Xcc B100 $XopD_{XccB100}$ fusion proteins

Two fusion proteins were constructed that contained the N-terminus of XopD and the C-terminus of $XopD_{XccB100}$: XopDvc1 ($XopD_{1-457}$-$XopD_{XccB100\ 533–801}$) and XopDvc2 ($XopD_{1-379}$-$XopD_{XccB100\ 399–801}$). The 1-kb *Eco*RI-*Xba*I fragment of the Xcv 85-10 *xopD* gene in pVSP61(*lacZ promoter-xopD-His*) was replaced with a 0.8-kb *Eco*RI-*Xba*I fragment of the *xopD*$_{XccB100}$ gene in pVSP61(*lacZ promoter-xopD*$_{XccB100}$*-His*), generating pVSP61(*lacZ promoter-xopDvc1-His*). The 1.2-kb *Stu*I-*Xba*I fragment of the Xcv 85-10 *xopD* gene in pVSP61(*lacZ promoter-xopD-His*) was replaced with the 1.2-kb *Stu*I-*Xba*I fragment of the *xopD*$_{XccB100}$ gene in pVSP61(*lacZ promoter-xopD*$_{XccB100}$*-His*), generating pVSP61(*lacZ promoter-xopDvc2-His*). The plasmids were each conjugated into Xcv Δ*xopD* and tested for complementation of the Δ*xopD* mutant phenotype in tomato leaves.

Xcv growth curves in tomato

To monitor Xcv growth *in planta*, VF36 tomato leaves were hand-inoculated by complete infiltration of the leaf tissue with a 1×10^5 cfu/mL suspension of bacteria in 10 mM $MgCl_2$ using a needleless syringe. Leaves of the same age on the same branch were used for each experimental test. Plants were kept under 16 h light/day at 28 °C. Two leaf discs (0.25cm^2) per treatment per time point were ground in 10 mM $MgCl_2$, diluted and spotted onto NYGA plates in triplicate to determine the bacterial load. Three biological replicates (i.e. three plants) were used and the average bacterial titre ± standard deviation for the three experiments is reported. The experiment was repeated at least three times.

Protein extraction and immunoblot analysis

Protein pellets were washed in 1 M Tris and resuspended in 8 M urea sample buffer. Protein was extracted from plant cells as described previously (Mudgett and Staskawicz, 1999). Proteins separated by SDS-PAGE and transferred to nitrocellulose were detected by ECL chemiluminescence (GE Healthcare, Piscataway, NJ, USA) using anti-HA sera (Covance, Emeryville, CA, USA), anti-His sera (Qiagen) or anti-green fluorescent protein (GFP) antisera (Covance) and horseradish peroxidase-conjugated secondary antibodies (Bio-Rad).

ACKNOWLEDGEMENTS

The authors thank Alfred Pühler, David Stahl and Brian Staskawicz for strains, Sharon Long (Stanford University, Stanford) and David Ehrhardt (Carnegie Institution, Stanford) for the use of

equipment, Abrahim El Gamal (Stanford University, Stanford) for technical assistance and Ken Frame (Stanford University, Stanford) for critical discussions. M.B.M. was supported by the National Institutes of Health Grant 2R01 GM068886-06A1 and the National Science Foundation Grant IOS-0821801.

REFERENCES

Aguilar, O.M., Kapp, D. and Pühler, A. (1985) Characterization of a *Rhizobium meliloti* fixation gene (*fixF*) located near the common nodulation region. *J. Bacteriol.* **164**, 245–254.

Almeida, N.F., Yan, S., Lindeberg, M., Studholme, D.J., Schneider, D.J., Condon, B., Liu, H.J., Viana, C.J., Warren, A., Evans, C., Kemen, E., MacLean, D., Angot, A., Martin, G.B., Jones, J.D., Collmer, A., Setubal, J.C. and Vinatzer, B.A. (2009) A draft genome sequence of *Pseudomonas syringae* pv. *tomato* T1 reveals a type III effector repertoire significantly divergent from that of *Pseudomonas syringae* pv. *tomato* DC3000. *Mol. Plant–Microbe Interact.* **22**, 52–62.

Altschul, S.F., Gish, W., Miller, W., Myers, E.W. and Lipman, D.J. (1990) Basic local alignment search tool. *J. Mol. Biol.* **215**, 403–410.

Bonas, U., Schulte, R., Fenselau, S., Minsavage, G.V., Staskawicz, B.J. and Stall, R.E. (1991) Isolation of a gene cluster from *Xanthomonas campestris* pv. *vesicatoria* that determines pathogenicity and the hypersensitive response on pepper and tomato. *Mol. Plant–Microbe Interact.* **4**, 81–88.

Castaneda, A., Reddy, J.D., El-Yacoubi, B. and Gabriel, D.W. (2005) Mutagenesis of all eight avr genes in *Xanthomonas campestris* pv. *campestris* had no detected effect on pathogenicity, but one avr gene affected race specificity. *Mol. Plant–Microbe Interact.* **18**, 1306–1317.

Chosed, R., Tomchick, D.R., Brautigam, C.A., Mukherjee, S., Negi, V.S., Machius, M. and Orth, K. (2007) Structural analysis of *Xanthomonas* XopD provides insights into substrate specificity of ubiquitin-like protein proteases. *J. Biol. Chem.* **282**, 6773–6782.

Dow, J.M., Crossman, L., Findlay, K., He, Y.Q., Feng, J.X. and Tang, J.L. (2003) Biofilm dispersal in *Xanthomonas campestris* is controlled by cell-cell signaling and is required for full virulence to plants. *Proc. Natl. Acad. Sci. USA*, **100**, 10995–11000.

Hotson, A., Chosed, R., Shu, H., Orth, K. and Mudgett, M.B. (2003) *Xanthomonas* type III effector XopD targets SUMO-conjugated proteins *in planta*. *Mol. Microbiol.* **50**, 377–389.

Innes, R.W., Bent, A.F., Kunkel, B.N., Bisgrove, S.R. and Staskawicz, B.J. (1993) Molecular analysis of avirulence gene avrRpt2 and identification of a putative regulatory sequence common to all known *Pseudomonas syringae* avirulence genes. *J. Bacteriol.* **175**, 4859–4869.

Jones, J.B., Bouzar, H., Stall, R.E., Almira, E.C., Roberts, P.D., Bowen, B.W., Sudberry, J., Strickler, P.M. and Chun, J. (2000) Systematic analysis of xanthomonads (*Xanthomonas* spp.) associated with pepper and tomato lesions. *Int. J. Syst. Evol. Microbiol.* **50**, 1211–1219.

Jones, J.B., Gitaitis, R.D. and Schaad, N.W. (2001) *Acidovorax* and *Xylophilis*. In: *Laboratory Guide for Identification of Plant Pathogenic Bacteria* (Schaad, N.W., Jones, J.B. and Chun, W., eds), pp. 121–138. St. Paul, MN: APS Press.

Kamiunten, H. (1990) Loss of a plasmid in *Pseudomonas syringae* pv. *eriobotryae* is correlated with change of symptoms. *Ann. Phytopathol. Soc. Jpn.* **56**, 645–650.

Kamiunten, H. (1999) Isolation and characterization of virulence gene *psvA* on a plasmid of *Pseudomonas syringae* pv. *eriobotryae*. *Ann. Phytopathol. Soc. Jpn.* **65**, 501–509.

Kay, S., Hahn, S., Marois, E., Hause, G. and Bonas, U. (2007) A bacterial effector acts as a plant transcription factor and induces a cell size regulator. *Science*, **318**, 648–651.

Kazan, K. (2006) Negative regulation of defence and stress genes by EAR-motif-containing repressors. *Trends Plant Sci.* **11**, 109–112.

Kim, N.H., Choi, H.W. and Hwang, B.K. (2010) *Xanthomonas campestris* pv. *vesicatoria* effector AvrBsT induces cell death in pepper, but suppresses defense responses in tomato. *Mol. Plant–Microbe Interact.* **23**, 1069–1082.

Kim, J.G., Li, X., Roden, J.A., Taylor, K.W., Aakre, C.D., Su, B., Lalonde, S., Kirik, A., Chen, Y., Baranage, G., McLane, H., Martin, G.B. and Mudgett, M.B. (2009) *Xanthomonas* T3S effector XopN suppresses PAMP-triggered immunity and interacts with a tomato atypical receptor-like kinase and TFT1. *Plant Cell*, **21**, 1305–1323.

Kim, J.G., Taylor, K.W., Hotson, A., Keegan, M., Schmelz, E.A. and Mudgett, M.B. (2008) XopD SUMO protease affects host transcription, promotes pathogen growth, and delays symptom development in *Xanthomonas*-infected tomato leaves. *Plant Cell*, **20**, 1915–1929.

Kirik, A. and Mudgett, M.B. (2009) SOBER1 phospholipase activity suppresses phosphatidic acid accumulation and plant immunity in response to bacterial effector AvrBsT. *Proc. Natl. Acad. Sci. USA*, **106**, 20532–20537.

Koebnik, R., Kruger, A., Thieme, F., Urban, A. and Bonas, U. (2006) Specific binding of the *Xanthomonas campestris* pv. *vesicatoria* AraC-type transcriptional activator HrpX to plant-inducible promoter boxes. *J. Bacteriol.* **188**, 7652–7660.

Marois, E., Van den Ackerveken, G. and Bonas, U. (2002) The *Xanthomonas* type III effector protein AvrBs3 modulates plant gene expression and induces cell hypertrophy in the susceptible host. *Mol. Plant–Microbe Interact.* **15**, 637–646.

Mudgett, M.B. and Staskawicz, B.J. (1999) Characterization of the *Pseudomonas syringae* pv. *tomato AvrRpt2* protein: demonstration of secretion and processing during bacterial pathogenesis. *Mol. Microbiol.* **32**, 927–941.

Mukherjee, S., Keitany, G., Li, Y., Wang, Y., Ball, H.L., Goldsmith, E.J. and Orth, K. (2006) *Yersinia* YopJ acetylates and inhibits kinase activation by blocking phosphorylation. *Science*, **312**, 1211–1214.

Nissan, G., Manulis-Sasson, S., Weinthal, D., Mor, H., Sessa, G. and Barash, I. (2006) The type III effectors HsvG and HsvB of gall-forming *Pantoea agglomerans* determine host specificity and function as transcriptional activators. *Mol. Microbiol.* **61**, 1118–1131.

Noël, L., Thieme, F., Nennstiel, D. and Bonas, U. (2002) Two novel type III-secreted proteins of *Xanthomonas campestris* pv. *vesicatoria* are encoded within the hrp pathogenicity island. *J. Bacteriol.* **184**, 1340–1348.

Ohta, M., Matsui, K., Hiratsu, K., Shinshi, H. and Ohme-Takagi, M. (2001) Repression domains of class II ERF transcriptional repressors share an essential motif for active repression. *Plant Cell*, **13**, 1959–1968.

Qian, W., Jia, Y., Ren, S.-X., He, Y.-Q., Feng, J.-X., Lu, L.-F., Sun, Q., Ying, G., Tang, D.-J., Tang, H., Wu, W., Hao, P., Wang, L., Jiang, B.-L., Zeng, S., Gu, W.-Y., Lu, G., Rong, L., Tian, Y., Yao, Z., Fu, G., Chen, B., Fang, R., Qiang, B., Chen, Z., Zhao, G.-P., Tang, J.-L. and He, C. (2005) Comparative and functional genomic analyses of the pathogenicity of phytopathogen *Xanthomonas campestris* pv. *campestris*. *Genome Res.* **15**, 757–767.

Roden, J., Eardley, L., Hotson, A., Cao, Y. and Mudgett, M.B. (2004) Characterization of the *Xanthomonas* AvrXv4 effector, a SUMO protease translocated into plant cells. *Mol. Plant–Microbe Interact.* **17**, 633–643.

Römer, P., Hahn, S., Jordan, T., Strauss, T., Bonas, U. and Lahaye, T. (2007) Plant pathogen recognition mediated by promoter activation of the pepper Bs3 resistance gene. *Science*, **318**, 645–648.

Rytkonen, A., Poh, J., Garmendia, J., Boyle, C., Thompson, A., Liu, M., Freemont, P., Hinton, J.C. and Holden, D.W. (2007) SseL, a *Salmonella* deubiquitinase required for macrophage killing and virulence. *Proc. Natl. Acad. Sci. USA*, **104**, 3502–3507.

da Silva, A.C., Ferro, J.A., Reinach, F.C., Farah, C.S., Furlan, L.R., Quaggio, R.B., Monteiro-Vitorello, C.B., Van Sluys, M.A., Almeida, N.F., Alves, L.M., do Amaral, A.M., Bertolini, M.C., Camargo, L.E., Camarotte, G., Cannavan, F., Cardozo, J., Chambergo, F., Ciapina, L.P., Cicarelli, R.M., Coutinho, L.L., Cursino-Santos, J.R., El-Dorry, H., Faria, J.B., Ferreira, A.J., Ferreira, R.C., Ferro, M.I., Formighieri, E.F., Franco, M.C., Greggio, C.C., Gruber, A., Katsuyama, A.M., Kishi, L.T., Leite, R.P., Lemos, E.G., Lemos, M.V., Locali, E.C., Machado, M.A., Madeira, A.M., Martinez-Rossi, N.M., Martins, E.C., Meidanis, J., Menck, C.F., Miyaki, C.Y., Moon, D.H., Moreira, L.M., Novo, M.T., Okura, V.K., Oliveira, M.C., Oliveira, V.R., Pereira, H.A., Rossi, A., Sena, J.A., Silva, C., de Souza, R.F., Spinola, L.A., Takita, M.A., Tamura, R.E., Teixeira, E.C., Tezza, R.I., Trindade dos Santos, M., Truffi, D., Tsai, S.M., White, F.F., Setubal, J.C. and Kitajima,

J.P. (2002) Comparison of the genomes of two *Xanthomonas* pathogens with differing host specificities. *Nature*, **417**, 459–463.

Sambrook, J., Fritsch, E.F. and Maniatis, T. (1989) *Molecular Cloning: A Laboratory Manual*. Cold Spring Harbor, NY: Cold Spring Harbor Laboratory Press.

Stall, R. (1995) Xanthomonas campestris pv. vesicatoria. In: *Pathogenesis and Host Specificity in Plant Diseases: Histopathological, Biochemical, Genetic, and Molecular Bases* (Singh, R.P. and Kohmoto, K., eds), pp. 167–184. New York: Pergamon/Elsevier.

Staskawicz, B.J., Mudgett, M.B., Dangl, J.L. and Galan, J.E. (2001) Common and contrasting themes of plant and animal diseases. *Science*, **292**, 2285–2289.

Szczesny, R., Buttner, D., Escolar, L., Schulze, S., Seiferth, A. and Bonas, U. (2010) Suppression of the AvrBs1-specific hypersensitive response by the YopJ effector homolog AvrBsT from *Xanthomonas* depends on a SNF1-related kinase. *New Phytol.* **187**, 1058–1074.

Tai, T.H., Dahlbeck, D., Clark, E.T., Gajiwala, P., Pasion, R., Whalen, M.C., Stall, R.E. and Staskawicz, B.J. (1999) Expression of the Bs2 pepper gene confers resistance to bacterial spot disease in tomato. *Proc. Natl. Acad. Sci. USA*, **96**, 14153–14158.

Tamura, K., Dudley, J., Nei, M. and Kumar, S. (2007) MEGA4: Molecular Evolutionary Genetics Analysis (MEGA) Software Version 4.0. *Mol. Biol. Evol.* **24**, 1596–1599.

Thieme, F., Koebnik, R., Bekel, T., Berger, C., Boch, J., Buttner, D., Caldana, C., Gaigalat, L., Goesmann, A., Kay, S., Kirchner, O., Lanz, C., Linke, B., McHardy, A.C., Meyer, F., Mittenhuber, G., Nies, D.H., Niesbach-Klosgen, U., Patschkowski, T., Ruckert, C., Rupp, O., Schneiker, S., Schuster, S.C., Vorholter, F.J., Weber, E., Puhler, A., Bonas, U., Bartels, D. and Kaiser, O. (2005) Insights into genome plasticity and pathogenicity of the plant pathogenic bacterium *Xanthomonas campestris* pv. *vesicatoria* revealed by the complete genome sequence. *J. Bacteriol.* **187**, 7254–7266.

Thompson, J.D., Gibson, T.J., Plewniak, F., Jeanmougin, F. and Higgins, D.G. (1997) The CLUSTAL_X windows interface: flexible strategies for multiple sequence alignment aided by quality analysis tools. *Nucleic Acids Res.* **25**, 4876–4882.

Turner, P., Barber, C. and Daniels, M. (1984) Behaviour of the transposons Tn*5* and Tn*7* in *Xanthomonas campestris* pv. *campestris*. *Mol. Gen. Genet.* **195**, 101–107.

Vorhölter, F.J., Schneiker, S., Goesmann, A., Krause, L., Bekel, T., Kaiser, O., Linke, B., Patschkowski, T., Ruckert, C., Schmid, J., Sidhu, V.K., Sieber, V., Tauch, A., Watt, S.A., Weisshaar, B., Becker, A., Niehaus, K. and Pühler, A. (2008) The genome of *Xanthomonas campestris* pv. *campestris* B100 and its use for the reconstruction of metabolic pathways involved in xanthan biosynthesis. *J. Biotechnol.* **134**, 33–45.

Wengelnik, K., Rossier, O. and Bonas, U. (1999) Mutations in the regulatory gene hrpG of *Xanthomonas campestris* pv. *vesicatoria* result in constitutive expression of all hrp genes. *J. Bacteriol.* **181**, 6828–6831.

White, F.F., Potnis, N., Jones, J.B. and Koebnik, R. (2009) The type III effectors of *Xanthomonas*. *Mol. Plant Pathol.* **10**, 749–766.

SUPPORTING INFORMATION

Additional Supporting Information may be found in the online version of this article:

Figure S1 Expression level of XopD and XopD-like proteins in *Xanthomonas campestris* pv. *vesicatoria* (Xcv) ΔxopD cell extracts. Lane 1, Xcv wt (vector). Lane 2, Xcv Δ*xopD* (vector). Lane 3, Xcv Δ*xopD* (XopD-His). Lane 4, Xcv Δ*xopD* ($XopD_{216–760}$-His). Lane 5, Xcv Δ*xopD* ($XopD_{XccB100}$-His). Lane 6, Xcv Δ*xopD* ($PsvA_{Xcc8004}$-His). Lane 7, Xcv Δ*xopD* ($XopD_{Aac}$-His). Lane 8, Xcv Δ*xopD* (XopDvc1-His). Lane 9, Xcv Δ*xopD* (XopDvc2-His). Each gene was cloned into pVSP61 for constitutive expression by the *lacZ* promoter. Plasmids were conjugated into the Xcv Δ*xopD* null mutant and the exconjugants were analysed for protein expression. Cells were grown in nutrient yeast glycerol agar (NYGA) and lysed in urea sample buffer. Proteins were detected by protein gel blot analysis using anti-His sera. Protein standards (STD) are shown on the left in kilodaltons. The expected molecular weights for each protein are as follows: XopD-His, 86.5 kDa; $XopD_{216–760}$-His, 62.2 kDa; $XopD_{XccB100}$-His, 89.9 kDa; $PsvA_{Xcc8004}$-His, 50.5 kDa; $XopD_{Aac}$-His, 87.9 kDa; XopDvc1-His, 82.9 kDa; Xopvc2-His, 88.9 kDa.

FigureS2 Protein gel blot analysis of *Nicotiana benthamiana* leaves inoculated with the *Agrobacterium tumefaciens* strains used in Fig. 3A. Lane 1, vector. Lane 2, XopD-His. Lane 3, XopD(C685A)-His. Lane 4, $XopD_{216–760}$-His. Lane 5, $PsvA_{Xcc8004}$-His. Lane 6, $XopD_{XccB100}$-His. Lane 7, $XopD_{Aac}$-His. Leaves were hand-infiltrated with a suspension of 6×10^8 cells/mL of each strain. After 48 h, total protein was extracted and analysed by protein gel blot analysis using anti-His sera. Protein standards (STD) are shown on the left in kilodaltons. Expected protein molecular weights: XopD-His, 86.5 kDa; XopD(C685A)-His, 86.5 kDa; $XopD_{216–760}$-His, 62.2 kDa; $PsvA_{Xcc8004}$-His, 50.5 kDa; $XopD_{XccB100}$-His, 89.9 kDa; $XopD_{Aac}$-His, 87.9 kDa.

Figure S3 Protein gel blot analysis of *Nicotiana benthamiana* leaves inoculated with the *Agrobacterium tumefaciens* strains used in Fig. 3B. Lane 1, yellow fluorescent protein (YFP). Lane 2, YFP-$XopD_{216–760}$. Lane 3, YFP-XopD. Lane 4, YFP-$PsvA_{Xcc8004}$. Lane 5, YFP-$XopD_{XccB100}$. Lane 6, YFP-$XopD_{Aac}$. Leaves were hand-infiltrated with a suspension of 6×10^8 cells/mL of each strain. After 60 h, total protein was extracted and analysed by protein gel blot analysis using anti-green fluorescent protein (GFP) sera. Protein standards (STD) are shown on the left in kilodaltons. Expected protein molecular weights: YFP, 30.4 kDa; YFP-$XopD_{216–760}$, 91.4 kDa; YFP-XopD, 115.8 kDa; YFP-$PsvA_{Xcc8004}$, 79.8 kDa; YFP-$XopD_{XccB100}$, 119.2 kDa; YFP-$XopD_{Aac}$, 117.2 kDa.

Figure S4 Growth and phenotype of the *Xanthomonas campestris* pv. *campestris* (Xcc) B100 $xopD_{XccB100}$ null mutant in host leaves. (A) Black rot symptoms caused by Xcc B100, Xcc B100 Δ*hrcV* and Xcc B100 Δ$xopD_{XccB100}$ strains on infected radish (cv. Champion) leaves. Leaves were inoculated by the leaf clipping method (Dow *et al*., 2003) with a 1×10^8 cells/mL suspension of bacteria in 10 mM $MgCl_2$. Leaves were photographed at 12 days post-inoculation. The experiments were repeated twice with similar results. (B) Lesion length caused by Xcc B100, Xcc B100 Δ*hrcV* and Xcc B100 Δ$xopD_{XccB100}$ strains in radish leaves. Data points represent the mean lesion length (mm) ± standard deviation (SD) of 15 radish leaves. Error bars indicate SD. (C) Growth of Xcc B100 (white bars) and Xcc B100 Δ$xopD_{XccB100}$ (grey bars) in *Arabidopsis thaliana* Col-0 leaves. Leaves were hand-inoculated with a 2×10^5 cells/mL suspension of bacteria. Data points represent mean $\log_{10}$ colony-forming units (cfu)/cm^2 ± SD of three plants. Error bars indicate SD. The experiments were repeated three times with similar results. (D) Growth of Xcc B100 (white bars) and Xcc B100 Δ$xopD_{XccB100}$ (black bars) in *Nicotiana benthamiana* leaves. Leaves were hand-inoculated with a 2×10^5 cells/mL suspension of bacteria. Data points represent mean $\log_{10}$ cfu/cm^2 ± SD of three plants. Error bars indicate SD. The experiments were repeated twice with similar results.

Figure S5 Comparison of XopD and $XopD_{XccB100}$ protein sequences. (A) Schematic diagram of xopD and $XopD_{XccB100}$. Percentage amino acid sequence identity is noted for the adjacent highlighted grey regions. (B) Amino acid sequence comparison between the N-terminal amino acid residues of XopD (1–379 amino acids) from Xcv 85-10 and $XopD_{XccB100}$ (1–398 amino acids) from Xcc B100. Proteins were aligned using the CLUSTALX program. Dashes (-) indicate gaps introduced into the XopD sequence to maximize the alignment between the two protein sequences.

Please note: Wiley-Blackwell are not responsible for the content or functionality of any supporting materials supplied by the authors. Any queries (other than missing material) should be directed to the corresponding author for the article.